Available online at www.sciencedirect.com
SCIENCE DIRECT
Catalysis Today 111 (2006) 34–43
CATALYSIS TODAY
www.elsevier.com/locate/cattod

From atom-resolved scanning tunneling microscopy (STM) studies to the design of new catalysts

Jeppe V. Lauritsen, Ronnie T. Vang, Flemming Besenbacher *

Interdisciplinary Nanoscience Center (iNANO) and Department of Physics and Astronomy, University of Aarhus, DK-8000 Aarhus C, Denmark

Available online 28 November 2005

Abstract

The scanning tunneling microscope (STM) is today established as a unique tool for resolving the atomic-scale structure of surfaces. STM studies of model systems relevant to heterogeneous catalysis have made it possible to address and resolve many important, fundamental questions related to catalytic processes by imaging, in direct space, the atomic-scale structure of catalytically relevant model systems, e.g. adsorbate-covered single crystal surfaces or nanoclusters supported either on metals or oxide surfaces. These studies are normally carried out under well-controlled vacuum or pressure conditions. Here we discuss three recent STM studies of model catalyst systems, all illustrating how the insight gained from fundamental studies of idealized model systems has been successfully linked to studies on real catalyst systems operating under realistic conditions, and how this interplay has facilitated the development of new and superior high surface area catalysts.
© 2005 Elsevier B.V. All rights reserved.

Keywords: Model catalyst; Scanning tunneling microscopy; STM; Steam reforming; Hydrodesulfurization; Nanoclusters; MoS_2

1. Introduction

The need for a better understanding of heterogeneous catalysis has led to the development of a number of specialized experimental techniques, that provide detailed structural and chemical insight into either complex catalysts or simpler model systems. The multitude of techniques used in catalysis research today [1–4] are nearly all developed as general solid-state or surface science techniques with limited direct application for the study of complex catalysts. Major developments and refinements of techniques like X-ray absorption spectroscopy, X-ray diffraction, infrared spectroscopy and high-resolution electron spectroscopy have made it possible today to achieve a relatively good understanding of a number of different catalyst systems. However, traditional diffraction and spectroscopic methods are, generally, averaging techniques where the information about individual atoms and particles is difficult to extract, and although these techniques have given unprecedented new insight into both model catalysts of, e.g. supported nanoclusters and technical catalysts, they are thus not able to resolve the detailed atomic-scale structure of catalytically active sites such as atomic defects or edge sites, which often determine the catalytic activity.

The scanning tunneling microscope (STM) technique, on the contrary, is a direct real-space, local probe technique that is capable of resolving the atomic-scale structure of surfaces with atomic resolution. What has fascinated many scientists, and what sets the STM apart from most other surface science techniques, is its ability to investigate, atom-by-atom, the electronic and geometric structure of surface structures. STM therefore stands out as a unique and versatile tool for exploring the direct-space structure of conducting surfaces, supported nanoclusters and adsorbates on these. Since the development of the STM 25 years ago [5], it has matured tremendously and from being a complicated, highly specialized physics instrument, sensitive to vibrations and drift, the STM has developed into a compact and stable analytical tool, which now finds widespread application in a number of disciplines. The confidence gained in the operation and interpretation of STM results has led to a situation where we can now apply STM to solve various problems related to the structure and reactivity of surfaces relevant for heterogeneous catalysis [6–8]. Since it also resolves signatures of adsorbed particles (sometimes even with high temporal resolution), it has become an outstanding

* Corresponding author. Tel.: +45 8942 3604; fax: +45 8942 3690.
E-mail address: fbe@inano.dk (F. Besenbacher).

0920-5861/$ – see front matter © 2005 Elsevier B.V. All rights reserved.
doi:10.1016/j.cattod.2005.10.015

tool for monitoring atomic and molecular dynamics and chemical reactions on surfaces with direct relevance to catalysis [9,10]. The ability of the STM to achieve atom-resolved real-space images of localized regions of the surface has thus often revealed unprecedented new insight on catalytically active sites and, in particular, emphasized the catalytic importance of edges, kinks, atom vacancies or other defects, which are often difficult or impossible to detect when using other techniques [10–12].

The STM technique, as such, is conceptually very simple and relies on the measurement of a small tunneling current floating between an atomically sharp metal tip, which is raster-scanned at a sub-nanometer distance to the surface to be imaged (see Refs. [6,8] for a detailed description). In the so-called constant current mode of the STM, the sharp tip traces the surface structure in a way that keeps the detected tunnel current at a constant value (around 1 nA), and the movement of the tip is recorded to produce a map of the underlying structures thus revealing atomic steps, clusters and, ultimately, the position of single atoms and molecules. Since STM is based on the tunneling of electron from tip to surface and vice versa, the electronic structure plays a role in the contrast formation in atom-resolved images and great care must be taken in order to interpret STM images. Specifically, the STM images reflect to a first approximation contours of surface local density of electronic states (LDOS), and in the cases where the electronic structure exhibits marked variations as compared to the geometrical structure, it is not straightforward to interpret the STM images. It is thus generally not correct to assume that STM images reflect a purely geometrical representation of the surface atomic structure, and in general STM images show a rather complicated variation of geometrical and electronic surface structure. Preferably the STM observations should be combined with theoretical simulations of STM images, and thus very detailed information on the atomic-scale surface structure can indeed be obtained.

Since utmost stability is required for the successful operation of STM and the fact that a tip has to sweep a surface at sub-nanometer distance, it is evident that STM cannot be used to image catalyst nanoparticles supported on a real, porous and often insulating carrier. The STM requires flat and conductive samples, and, like in most surface science techniques, the complexity of a catalyst is therefore stepwise broken down into simplified problems, that can be dealt with in detail in STM model studies. Typically the unsupported material is investigated in the form of single crystal surfaces, or, more elaborate model systems consisting of nano-particles deposited on a substrate may be synthesized, when there is a distinct relation between the catalytic properties and the size of the clusters. The STM thus offers a unique view of such structures on the atomic-scale, and it can undoubtedly give unprecedented new fundamental insight, which subsequently can trigger new ideas for the development of new and better catalysts. Here we discuss three such examples, where the full route is taken from STM studies of idealized model system to the synthesis of high surface area catalysts; an STM study of supported MoS_2 nanoclusters as a model catalyst for hydrodesulfurization/hydrotreating and two studies on the role of Ag and Au modifiers on Ni(1 1 1) as a model system for steam reforming catalysis.

2. Hydrodesulphurization model catalyst studied with STM

The MoS_2-based hydrodesulphurization (HDS) catalyst has been the subject of extensive studies using a large variety of different tools, and several extensive reviews on the subject exist [13–17]. A considerable effort has been aimed at relating fundamental characteristics such as catalyst activity and selectivity to microscopic properties, e.g. catalyst composition, electronic structure and geometric structure. In particular, in situ EXAFS studies and Mössbauer spectroscopy studies have provided information on the structure, and today the ''CoMoS'' model of Topsøe, Clausen and co-workers is widely accepted to describe the active structures in the catalysts. In the model, it is suggested that the active phase is present as supported single-layer MoS_2-like nano-clusters with a size of 10–20 Å under operating conditions, and that the promoting effect of Co in the CoMoS structures is caused by Co promoter atoms replacing Mo at positions near the edges of the MoS_2 clusters [18–21].

Despite the impressive number of studies of HDS catalysts, a series of fundamental questions remained, however, unanswered. Much of the controversy is directly related to the fact that the traditional spectroscopy-based techniques are not able to unequivocally map the real-space atomic structure of the few nanometer wide CoMoS nanoclusters. It was recognized early that only the edges of the S-Mo-S layers in MoS_2 are catalytically active [13,22], but in order to pinpoint and understand more precisely the active sites, it is necessary to obtain more detailed information on the atomic-scale structure of MoS_2 nanoclusters. For instance, what is the preferential morphology of the MoS_2 nanoclusters, which are the active edge structures, and what is the role of the promoters in CoMoS? To investigate these and a number of other issues related to the structure of the HDS catalyst, we have recently synthesized nanometer-sized MoS_2 nanoclusters and successfully used the STM to study directly the atomic-scale structure of individual MoS_2 and CoMoS nanoclusters.

The ability of the STM to achieve atom-resolved real-space images of the nanoclusters has made it possible, for the first time, to directly address the MoS_2 morphology and the structure of the catalytically important edges experimentally by synthesizing ensembles of single-layer MoS_2 or CoMoS nanoclusters on a flat Au(1 1 1) single crystal substrate as a realistic model system of the catalyst. Normally, oxide carriers are used in the industrial catalysts, but these are generally non-conducting and therefore unsuitable as supports for STM studies. The gold support is chosen since the close-packed Au(1 1 1) is rather inert, and we can therefore study the intrinsic properties of MoS_2, i.e. the MoS_2 nanoclusters are studied with a weak support-interaction. Furthermore, the Au(1 1 1) reconstructs in the characteristic herringbone pattern, which is used as a template for the synthesis of a highly dispersed ensemble of nanoclusters [23]. The detailed preparation

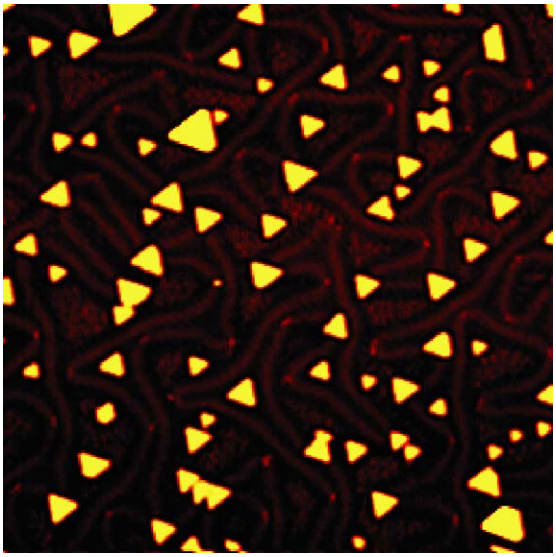

Fig. 1. STM image of MoS_2 nanoclusters synthesized on the Au(1 1 1) surface at 673 K in a sulfiding atmosphere. The size is 744 Å × 721 Å. Reproduced from [24].

method for the synthesis of MoS_2 and CoMoS nanoclusters supported on Au(1 1 1) is reported in [24,25]. As illustrated in Fig. 1, in the case of MoS_2, the clusters synthesized by this method are characterized by a high degree of dispersion and a fairly narrow size-distribution. The average size of the clusters is approximately 500 $Å^2$. This corresponds to a side length of ~30 Å, which matches well with the spatial extension of the active particles in typical HDS catalysts. A detailed analysis of STM images reveals that the morphology of the nanoclusters is also remarkably uniform with respect to shape, and as shown in the figure, we find that the triangular shape of MoS_2 clusters is strongly favoured under the conditions of the experiment. As a model system for the HDS catalyst, the MoS_2 clusters synthesized in this study therefore form a well-characterized reference for experiments elucidating details on the atomic structure of the catalytically active MoS_2 edge structures and their reactivity with adsorbed molecules.

An atomically resolved STM image of a triangular MoS_2 nanocluster consisting of a single S-Mo-S layer is illustrated in Fig. 2. The cluster is observed to be oriented with the (0 0 0 1) basal plane in parallel to the Au substrate and with the protrusions reflecting the hexagonally arranged S atoms in the topmost layer. At the edges, however, the protrusions are seen to be imaged *out* of registry with the basal plane S atoms. In fact, the protrusions are shifted exactly half a lattice constant along the edge, but retain their interatomic distance of 3.15 Å. The atomically resolved image thus provides the first direct information on the atomic-scale structure of the MoS_2 edges. The shifted registry along the edge could indicate that the catalytically active edges are severely reconstructed compared to a model based on bulk properties of MoS_2, but this is in fact not the case. As discussed briefly in Section 1, it is important to point out that STM images obtained in the constant current mode reflect contours of constant local density of states at the Fermi level measured at the position of the STM tip [26]. This implies that the contrast in STM images, in general, reflect a rather complicated convolution of geometric and electronic features of the surface/nanoclusters. This is in particular the case for materials that exhibit a band gap, e.g. metal oxides or sulfides. MoS_2 is a semiconductor with a band gap ~1.2 eV in the bulk form [27], and for the MoS_2 nanoclusters in the present study we indeed find that a purely geometrical model is not adequate to account for the STM images. Especially a pronounced bright *brim* of high electron state density is observed to extend all the way around the cluster edge adjacent to the edge protrusions in Fig. 2a. Furthermore, it is also seen from the atom-resolved images that the protrusions at the nanocluster edges are shifted exactly half a lattice constant along the edge. Rather than geometrical effects, these two signatures are attributed to an electronic effect probed by the

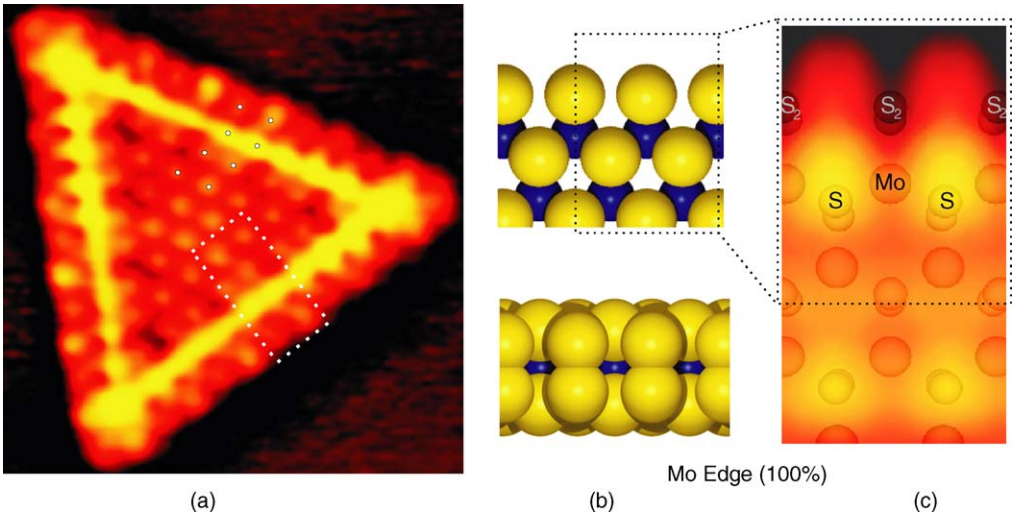

Fig. 2. (a) Atomically resolved STM image (V_t = 5.2 mV, I_t = 1.28 nA) of triangular, single-layer MoS_2 nanoclusters on Au(1 1 1). The size of the image is 41 Å × 42 Å. Adapted from [24]. (b) Side view and front view of the Mo edge fully saturated with S dimers. (c) Simulated STM image of a two-atom-wide section of the Mo edge with S dimers. The simulation is based on DFT calculations including the effect of the Au substrate (from [28]). The positions of the individual atoms in the simulated image are represented by shadowed atom balls (small: S, big: Mo). For clarity, the Au atoms of the support are omitted.

STM, reflecting the existence of localized electron states at the cluster perimeter, so-called *edge states*. In a successful collaboration with density functional theory (DFT) calculations by Bollinger et al. [28], it was possible to identify unambiguously these signatures in STM simulations, and we concluded that the MoS_2 nanoclusters expose the (1 0 $\bar{1}$ 0) Mo edges fully saturated with S_2 dimers (Fig. 2b). The calculations also directly show that the electronic structure near the Mo edges of the triangular MoS_2 nanoclusters is indeed significantly perturbed relative to the bulk, and they reveal that the edges are in fact metallic due to the existence of two distinct electronic edge states [28,29]. An STM simulation based on the Tersoff–Hamann model [26] (i.e. a contour map of the constant surface LDOS) shows that both the bright brim and the apparent shifted registry of the edge protrusions (Fig. 2c) can be traced back to the existence of the two edge states on the fully sulfided Mo edges, and the theory thus fully reproduces the experimentally observed features. Under the sulfiding conditions in the experiment, it is therefore concluded that triangular single-layer MoS_2 nanoclusters are terminated with the Mo edge fully covered with S dimers, and that the electronic structure of these edges is dominated by one-dimensional electronic "brim" states which give the edges a metallic character.

From a coordination chemistry point-of-view, fully sulfur-saturated edges, like the one in Fig. 2b, are not normally considered particularly reactive, but due to the metallic character of the edges we find evidence of a rather different chemistry than what has ordinarily been assumed. We investigate this by selectively adsorbing thiophene (C_4H_4S) molecules under ultra-high vacuum conditions on the MoS_2 clusters at different temperatures, and in this way we can mark the adsorption sites and map out the interaction strength. Specifically, we find that thiophene adsorbs non-dissociatively onto sites near the bright brims associated with a metallic one-dimensional edge state of MoS_2 at temperatures below 200 K, whereas we do not see thiophene adsorption on the inert (0 0 0 1) basal plane of the MoS_2 clusters [30]. The thiophene molecules thus seem to bind considerably stronger near the metallic edge state of the fully sulfided Mo edges than to internal regions of the MoS_2 basal plane, although the edges are still fully sulfur-saturated.

When the MoS_2 nanoclusters are treated with pre-dissociated hydrogen atoms, we observe an even stronger chemisorbed state of thiophene [31]. Fig. 3 shows an atom-resolved STM image of a triangular MoS_2 nanoclusters first exposed to atomic hydrogen and subsequently to thiophene. Adjacent to the edges, bean-like features that mark the position of thiophene related species are now visible. STM movies show that these molecules are mobile and diffuse along the cluster edges and that they therefore do not reflect molecules bound rigidly to a vacancy [31]. The molecules are identified as reaction intermediates resulting from a partial hydrogenation reaction occurring on the metallic brim states. The hydrogen that drives this reaction derives from H atoms adsorbed on the terminal S atoms on the edges from S–H groups [30], which are also observed under reaction conditions in the real catalyst. The combination of having hydrogen atoms adsorbed on the edges in the form of S–H groups and the unusual sites for thiophene adsorption on the metallic brim presents a favorable situation for a hydrogenation reaction. Comparing the experimental observed STM images with simulated STM images from extensive density functional theory (DFT) calculations, we conclude that the observed reaction intermediates are *cis*-but-2-ene-thiolates (C_4H_7S–) coordinated through the terminal sulfur

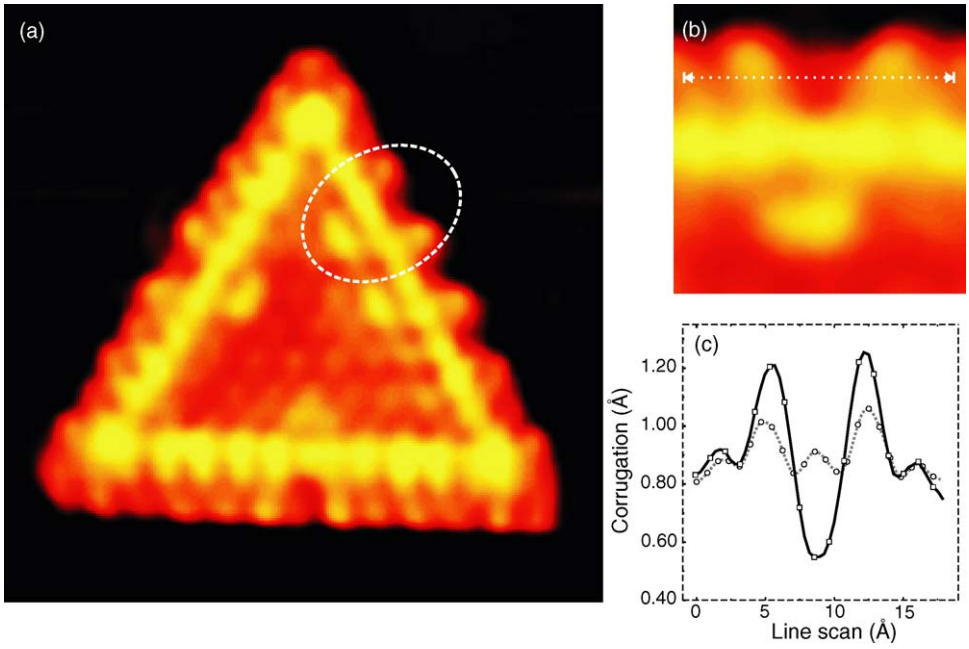

Fig. 3. (a) Atom-resolved STM image ($V_t = -331$ mV, $I_t = 0.50$ nA) of an atomic hydrogen pretreated MoS_2 cluster subsequently exposed to thiophene. Image dimensions are 50 Å × 54 Å. The dashed circle indicates the features, which are associated with individual, adsorbed molecules. (b) A close-up, which illustrates in detail the features associated with the adsorption of individual thiolate species at the edge of a MoS_2 nanocluster. (c) STM line scans along the edge protrusions of a cluster (black) corresponding to the line in (b). Line scan of an equal section of an unreacted, fully sulfided edge (gray dashed) is also shown. From Ref. [31].

atom to sites near the metallic brim. These species are formed by a sequential hydrogenation of one of the double bonds in thiophene by hydrogen adsorbed on the edges (from the S–H groups) followed by C–S bond cleavage. DFT calculations show that the reaction barrier associated with the rate-limiting step, the C–S bond-breaking, is actually quite modest ∼100 kJ/mol. The configuration observed in the STM image associated with a ring-opened structure is simply an ordinary thiol in which the S is much more reactive. The final extrusion of this S may proceed on sulfur vacancies. We have thus identified a route for an initial activation of a relatively inert S-bearing molecule like thiophene, and the reaction intermediates observed in the STM image may therefore be the result of an important first step of hydro-desulfurization. Interestingly, these processes take place on the metallic brim states of the fully saturated Mo edges, which have the ability to accept or donate electrons and thus act as catalytic sites just like ordinary metal surfaces.

Cobalt acts as a promoter for the catalysts, and also the edges of promoted CoMoS nanoclusters seem to possess metallic edge states. We therefore propose that metallic brim states may play a role also for the catalytic properties of the promoted phase. Fig. 4 shows an atomically resolved STM image of a single-layer CoMoS cluster formed by co-deposition of Mo and Co onto the Au substrate during exposure to an H_2S atmosphere and subsequent annealing. The main new finding is that the CoMoS nanoclusters adopt a *hexagonal* shape as opposed to the triangular morphology of unpromoted MoS_2. This change in the equilibrium shape is therefore attributed to the incorporation of cobalt into the MoS_2 structure, i.e. the formation of the CoMoS phase. The predominant hexagonal morphology implies that both fundamental types of low-indexed edge terminations of MoS_2 must be present, i.e. the Mo edge and the S edge. One edge type in the CoMoS is found to be similar to that observed for the MoS_2 triangles, with the edge protrusions clearly imaged *out* of registry with the lattice of S atoms on the basal plane and a bright brim along the edge. These edges are therefore identified as Mo edges, fully sulfided with two S dimers per Mo edge atom like in the triangles in Fig. 2a. From the symmetry of MoS_2, the other shorter edges are consequently attributed to S-type edges. On the basis of the detailed atomic-scale information provided by the STM images, a structural model of the CoMoS nanoclusters is proposed in which Co atoms have substituted Mo atoms along the S edges of hexagonally truncated nanoclusters. As depicted in the ball model in Fig. 4, a *tetrahedral* environment of the Co atoms is produced if the outermost protrusions are assumed to be S monomers, which agrees well with previously published EXAFS results on supported CoMoS catalysts [19,32–34] and previous DFT studies [35,36]. Interestingly, the promoted edges are in the STM images seen to exhibit an even brighter brim. This suggests that metallic brim states also exist in the promoted CoMoS structures, and in view of the result on the unpromoted clusters it is tentatively proposed that the promoted brim states may be connected to the higher catalytic activity of the Co-promoted phase.

Based on the new fundamental insight obtained and in particular the fact that the existence of reactive metallic sites near the edges was revealed, it was recently possible by the Haldor Topsøe company to synthesize and manufacture a novel generation of hydrotreating catalysts. The improved catalyst, which optimizes the number of brim sites and enhance the hydrogenation properties, was called the BRIM^{TM} catalysts inspired by the finding of electronic brim states in the STM images [37–39]. This shows that information gained in fundamental STM studies of idealized systems can generate the knowledge that may help to develop new and better industrial catalysts in the industry. It is doubtful whether any experimental technique other than STM could unequivocally point to the presence of electronic states on the edge of highly dispersed MoS_2 nanoclusters of this size and furthermore directly identify their role in the adsorption of relevant molecules.

3. Au/Ni surface alloy catalyst for steam reforming

Nickel is widely used as the active material in the industrially important steam reforming reaction. In the steam reforming process, natural gas (mainly CH_4) is reacted with

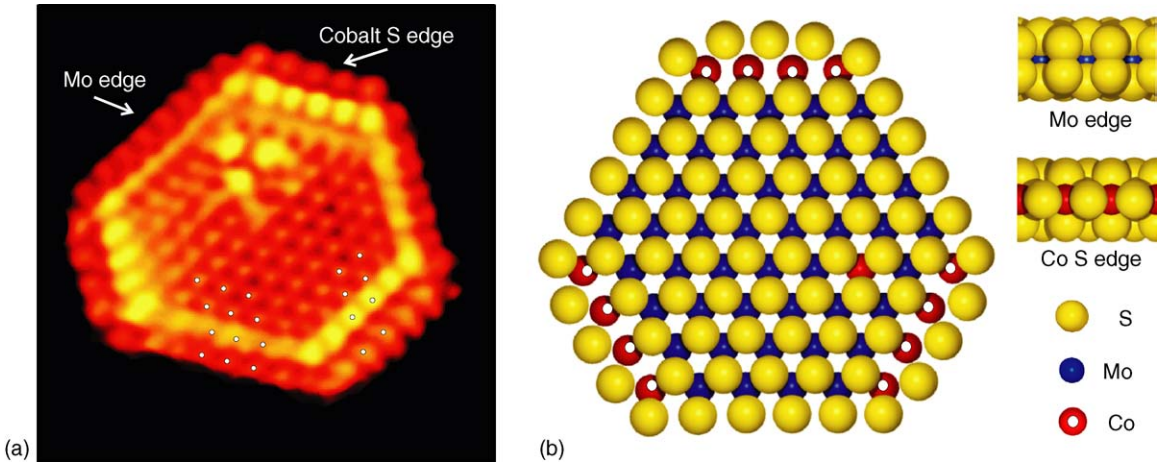

Fig. 4. (a) Atom-resolved STM image of a CoMoS nanocluster. Size is 51 Å × 52 Å and $V_t = -95.2$ mV, $I_t = 0.81$ nA (From Ref. [25]). Notice the very intense brim associated with the Co-substituted S edge (shorter edges). (b) Ball model of the proposed CoMoS structure. The CoMoS cluster is shown in top view exposing the unpromoted Mo edge and a Co-promoted S edge (Mo: dark, S: bright, Co: dark with spot). Also shown on the basal plane is a single Co inclusion. The Mo edge appears to be unaffected by Co and is shown in a side view ball model. The Co substituted S edge with a tetrahedral coordination of each edge Co is also shown.

steam (H_2O) to form synthesis gas, a mixture of H_2 and CO, and many of the challenges within the area of steam reforming have been discussed by Rostrup-Nielsen and co-workers [40–42]. A major technological challenge in the use of nickel catalysts in the steam reforming process, is that Ni is very active and also catalyzes the formation of graphite. This may lead to the growth of carbon filaments (so-called coking) and subsequently an accelerated deactivation and eventually complete breakdown of the catalyst [43,44]. Rostrup-Nielsen found that one possible way of circumventing the problem of graphite formation is to add minute amounts of H_2S to the feed gas [45]. The adsorbed S acts as a poison of the Ni catalyst, which, on one hand, inhibits the reforming process, but, on the other hand poisons the graphite formation even more, so that the overall gain is a improved selectivity and thus an extended life-cycle of the catalyst. This method was developed by Rostrup-Nielsen et al. into the so-called sulfur passivated reforming (SPARG) process [45]. It is, however, not an ultimate solution to the problem since sulfur is also a strong poison for most other transition-metal based catalysts used downstream to catalyze the formation of products. The presence of sulfur in the catalytic stream is therefore generally unwanted.

Another way of addressing the problem of graphite formation on nickel during the steam reforming reaction would be to alter the chemical properties of the nickel surface by, e.g., forming an alloy with another metal. It is well known that alloys in certain cases have superior catalytic properties compared to elementary metals [46,47], but typically focus has been on the class of binary metal systems that form ordered or random bulk alloys. However, another class of two-dimensional surface alloys has been revealed to exist for two-component metal systems that do not mix in the bulk, but which do form stable alloys in the outermost surface [48–50].

From STM studies [50] we have shown that the Au/Ni system belongs to this family of bulk-immiscible metals that form stable surface alloys. When Au is deposited on a Ni(1 1 1) surface, a surface alloy is formed: the Au atoms squeeze out Ni atoms and are substituted into Ni atom lattice positions as depicted in Fig. 5 in the atom-resolved STM images obtained after depositing Au atoms at 700 K [51]. By correlating the number of atoms imaged as depressions to the amount of evaporated Au, one sees that the Au atoms are imaged as depressions in the STM, although one would expect the Au atoms to protrude from the surface based on purely geometric arguments. This reflects the fact that STM images are, in general, a convolution of the geometric and the electronic structure, i.e. the LDOS at the positions of the Au atoms is lower than on the Ni sites.

The fact that a Au/Ni surface alloy is formed whereas no bulk 3D Au/Ni alloy exists (reflecting that the heat of solution of Au and Ni is large and positive, 27 kJ/mol) can be explained as follows. The Ni atoms in the surface layer are under-coordinated compared to the Ni atoms in the bulk. The Au atoms have a higher electron density than that of the Ni atoms, and when the Au atoms are alloyed into the surface layer, the neighboring Ni atoms will feel a higher electron density or, equivalently, a higher effective coordination number. The Au atoms that are alloyed into the surface layer thus help lowering the Ni surface energy. This simple reasoning is confirmed by extensive theoretical calculations [51].

Three fundamental findings originated the idea that the Au/Ni surface could have interesting catalytic properties for the steam reforming process. First, it was observed in the high-resolution STM images that the Au atoms alloyed into the Ni surface layer perturb the electronic structure of the nearby Ni atoms. Ni atoms with a neighboring Au atom are imaged brighter in the STM, and this effect is even more pronounced for those Ni atoms having two Au neighbors. DFT calculations confirm [52] that this effect cannot be explained by an outwards relaxation of the Ni atoms. Instead it reflects that the Au atoms perturbs the electronic structure of the neighboring Ni atoms, and thus we have basically three types of Ni atoms, Ni with atoms no Au nearest neighbors (nn), Ni atoms with one Au nn, and Au atoms with 2 Au nn. Second, DFT calculations showed that the Ni atoms with Au nearest neighbors have a higher activation barrier for hydrocarbon molecules such as CH_4.

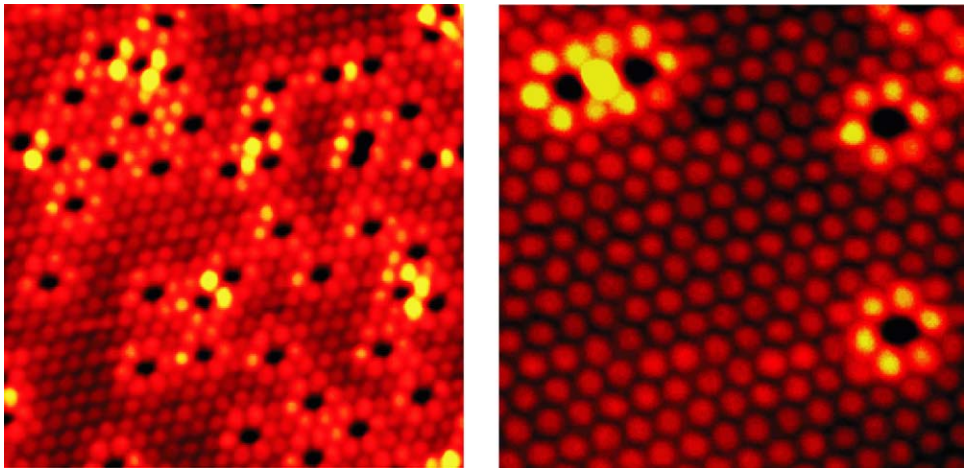

Fig. 5. Two STM images of the Ni(1 1 1) surface with 2% and 7% Au coverage, respectively. Au is imaged as dark depressions in the surface. The Ni atoms surrounding the Au appear brighter due to a local modification of the electronic structure, indicating a changed chemical activity of these. Adapted with permission from [51].

Finally, the DFT calculations (Fig. 6a) reveal that the tendency of the surface to bind carbon and form graphite is strongly impeded by the presence of the substituted Au in the topmost layer of the Ni(1 1 1) surface, and in particular this effect was found to be much more pronounced than the lowering of the activity towards activation of hydrocarbons [51].

These fundamental findings inspired the synthesis of a high surface area, $MgAl_2O_4$-supported Ni catalyst (with 16.5 wt.% Ni) which was modified with 0.3 wt.% Au [51]. By means of extended X-ray absorption fine structure spectroscopy (EXAFS) we verified that the Au is indeed alloyed into the first layer of the Ni catalyst. This high surface area Ni catalyst was then tested by measuring the activity for steam reforming of *n*-butane and comparing this to a similar measurement on a pure Ni catalyst; the results are shown in Fig. 6b. *n*-Butane was used to test the activity since it is known to give rise to the most severe graphite formation problems. Whereas the conventional Ni catalyst is deactivated rapidly due to the formation of graphite filaments, as confirmed by, e.g. electron microscopy, it was found that the conversion for the new catalyst with the Au/Ni nanoclusters is almost constant, i.e. for this new catalyst the graphite formation is significantly reduced. The results thus illustrate nicely that we also in this case, have reached a situation where fundamental insight into surface structure and reactivity has led to the design of a new steam reforming catalyst operating under technically relevant conditions.

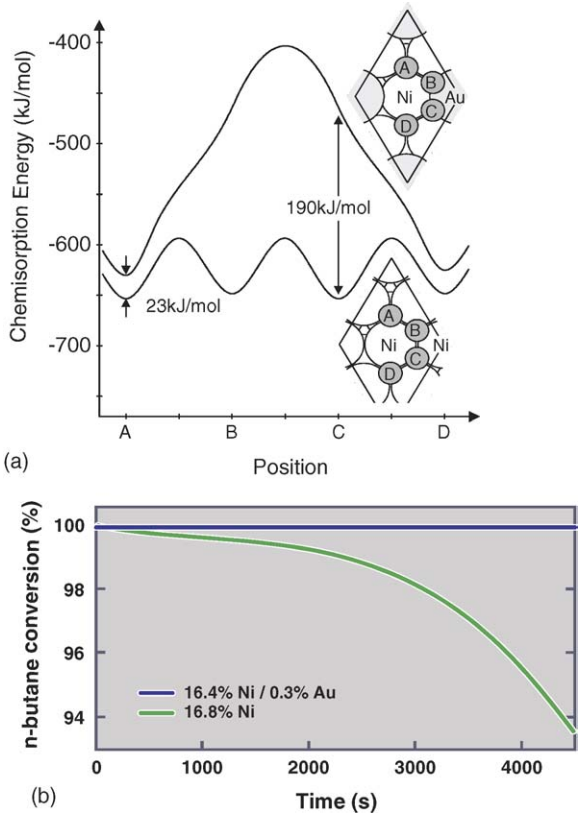

Fig. 6. (a) The probability of nucleation of graphite is determined by the stability of the adsorbed C atoms. The less stable the adsorbed C, the larger the tendency to react with adsorbed O to form CO and the lower the coverage. On the pure Ni(1 1 1) surface, the most stable adsorption site is the three-fold (hcp) site. The figure shows that three-fold sites next to a Au atom are seen to be completely unstable, and even the three-fold sites that are next-nearest neighbors to the Au atoms are substantially destabilized. (b) Conversion of *n*-butane as a function during steam reforming. The bright curve shows the conversion of the pure Ni catalyst, whereas the dark curve is for the Au/Ni catalyst. Adapted with permission from [51].

4. Selective site blocking by Ag atoms on Ni(1 1 1)

Whereas the *activity* often is the key parameter for the development of new catalysts, the *selectivity* is another and equally important factor for reactions with several possible reaction pathways. Very little information exists, however, on the ways in which the selectivity is controlled by special active sites, such as step edges or kinks [53–59]. To gain further insight and generate ideas of how to design new catalysts with improved selectivity, we recently investigated the initial steps of the decomposition of ethylene on Ni(1 1 1) surfaces. In the combined STM and DFT study, we have revealed interesting information on the role of the step edges for the rate of C–H and C–C bond-breaking. The results give important insight into the bond-breaking selectivity of the Ni catalyst between dissociation and primary dehydrogenation. This bond-breaking selectivity will eventually show up in the selectivity between the final products in, e.g., hydrogenolysis or dehydrogenation of hydrocarbons.

The most reactive sites on Ni(1 1 1) can be probed by dosing ethylene at the lowest temperature for which a reaction occurs. For room temperature exposure of ethylene we observed the formation of a brim of reaction products along the upper step edges of the Ni(1 1 1) surface, as can be seen in the STM image of Fig. 7a. The formation of this brim of ethylene decomposition products was found to be self-poisoning, i.e. the width of the brim did not increase with increasing ethylene dosing. This shows that the active sites for decomposing ethylene are blocked by the reaction products found at the brim, and we thus concluded that only the sites at the step edges of Ni(1 1 1) are active for ethylene decomposition at room temperature [60].

The STM data were complemented by DFT calculations in which the activation barriers were calculated for the two possible initial steps of the decomposition of ethylene: dissociation (C–C bond-breaking) and dehydrogenation (C–H bond-breaking). Step edges were introduced by performing the calculations both for the flat Ni(1 1 1) surface and for the stepped Ni(2 1 1) surface. The calculations showed that both energy barriers (dehydrogenation and dissociation) on the stepped surface were significantly lower than the lowest barrier (dehydrogenation) on the flat surface, consistent with the high reactivity of the step sites observed in the STM study. By comparing the step sites to terrace sites, the DFT calculations furthermore showed that the reduction in height of the activation barrier was much more pronounced for dissociation than for dehydrogenation, indicating that the selectivity of the Ni(1 1 1) surface towards ethylene dissociation/dehydrogenation, to a large extent, is determined by the ratio of step sites to terrace sites.

The selectivity of the Ni(1 1 1) may thus be controlled by modifying the number of free step sites. We therefore initiated

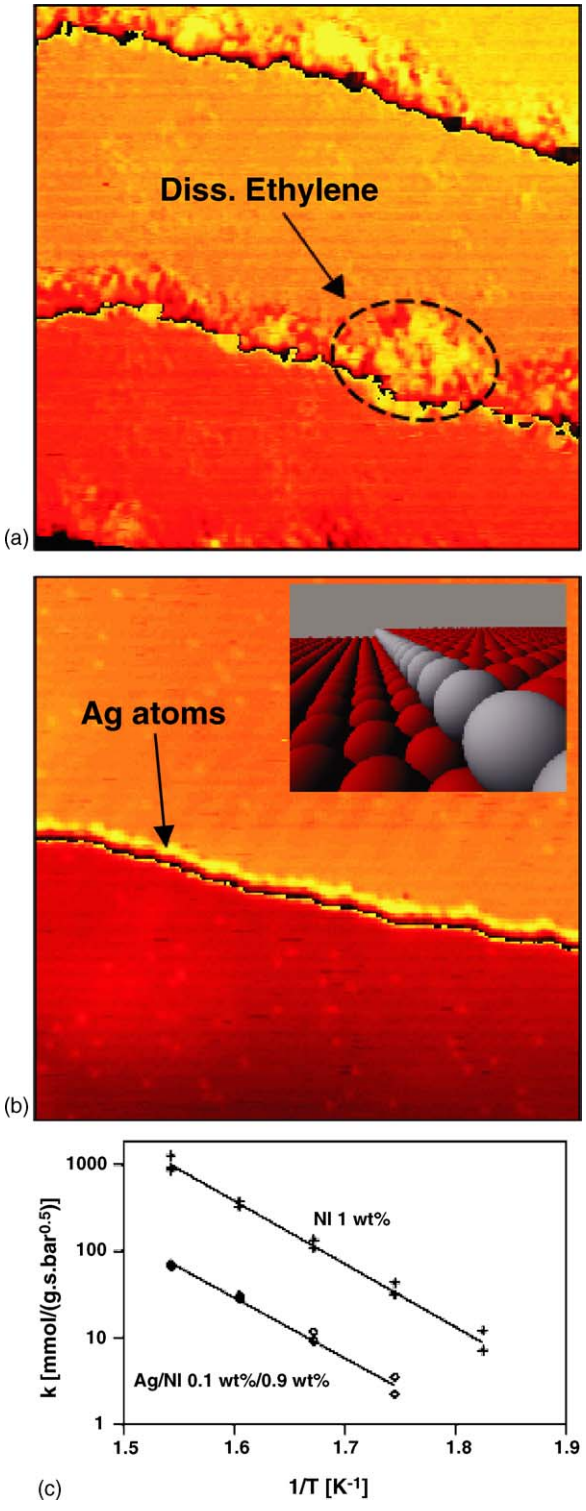

Fig. 7. (a) STM image (200 Å × 200 Å) of a Ni(1 1 1) surface after exposure to ethylene (10^{-8} Torr; 100 s) at room temperature. (b) STM image (400 Å × 400 Å) of a Ni(1 1 1) surface with the step edges blocked by Ag atoms. The small insert shows a ball model of a row of Ag atoms decorating a step edge on Ni(1 1 1). (c) Arrhenius plot of the rate constant for hydrogenolysis over $Ni/MgAl_2O_4$ and $Ag/Ni/MgAl_2O_4$. The rate (k) of ethane hydrogenolysis is one order of magnitude lower on the Ag/Ni catalyst as compared with the Ni catalyst, whereas the activation energy (slope of the Arrhenius curve) is similar.

STM experiments, in which the step edges were blocked by the addition of small amounts of Ag [60]. In previous STM studies we have found that when Ag is deposited on Ni(1 1 1) at room temperature, Ag preferentially nucleates and grows as islands at the step edges [49]. When these Ag islands on Ni(1 1 1) are post-annealed at 800 K, the Ag atoms become highly mobile and decorate all of the step edges of Ni(1 1 1), as seen in the STM image of Fig. 7b and illustrated by the inserted ball model. To test that the Ag atoms block the step edges, we subsequently exposed this Ag/Ni(1 1 1) surface to ethylene at room temperature and found by STM in this case no ethylene induced brim structure, neither at the step edges nor on the terraces. This clearly indicates that the step edge sites are indeed the active sites for the decomposition of ethylene at room temperature, and the experiments showed that the addition of silver effectively blocks these sites and changes the overall selectivity of the stepped Ni(1 1 1) surface.

To bridge the gap from the fundamental studies on model systems and exploit the new knowledge in a real catalyst, we have synthesized a new high surface area oxide-supported Ag/Ni catalyst [60]. The Ag-doped catalyst was tested for hydrogenolysis of ethane, which is the simplest possible reaction to probe the activity for C–C bond-breaking. The results are depicted in Fig. 7c, and it is seen that the design of the new Ag-modified catalyst has led to a decrease in the rate constant for ethane hydrogenolysis by approximately an order of magnitude. It is also seen that the activation energy (slope of the Arrhenius plots) is similar for the two catalysts, indicating that they have the same active sites. This was interpreted in the way that not all the step edges were blocked on the Ag/Ni catalysts, which is due to the complex structure of the highly dispersed and supported catalyst. The blocking of the dissociation pathway was attributed to the addition of silver to the Ni catalyst, and here the fundamental studies by STM have played a vital role in determining the role of step edges and providing clues on how to change the nature of these sites.

The very reactive step sites on Ni surfaces are also strongly involved in the formation of graphite during the steam reforming process as shown in recent STEM studies by Helveg et al. [43]. The poisoning effect of S utilized in the SPARG process may therefore also be speculated to relate to the step edges. We performed experiments with S on Ni(1 1 1) and especially studied its effect on the dissociation of CO. CO was used as the test molecule since it dissociates exclusively at the step edges and forms carbon structures, which are readily observed by STM (see Fig. 8a). When the Ni(1 1 1) surface was exposed to H_2S at 400 K we found that the sulfur atoms adsorbs preferentially along the step edges (Fig. 8b), and furthermore we found that CO did not dissociate on the Ni(1 1 1) surface when the step edges were decorated with S atoms. These observations are in agreement with the work of Goodman, who found that sulphur blocks the CO methanation reaction on Ni(1 0 0) [61]. Although these data are for CO dissociation, we expect that S will block the step edges for activation of any hydrocarbon molecule, and the step edges may thus play an important role in explaining the effect of S in the SPARG process. We have also shown that Au atoms block the step edges

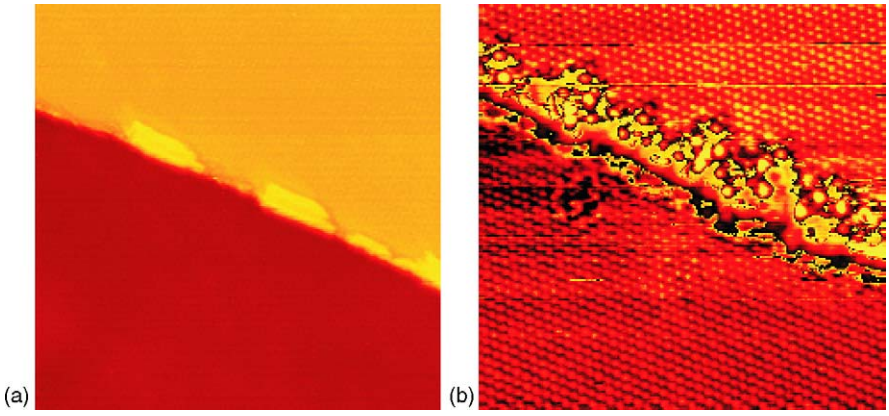

Fig. 8. (a) STM image (500 Å × 500 Å) of a Ni(1 1 1) surface showing the nucleation of carbon islands along the step edges after exposure to CO at 400 K. (b) STM image (100 Å × 100 Å) of single S atoms adsorbed at the step edge of a Ni(1 1 1) surface.

on the Au/Ni(1 1 1) surface alloy, and this may be part of the explanation of the improved carbon resistance of the Au/Ni alloy catalyst in the steam reforming process as discussed in the previous section.

5. Outlook and perspectives

In this article we have presented in a few examples on how studies of catalyst model systems have provided new insight that could be transferred to a real system and facilitate the synthesis of a new and better catalyst. This so-called *surface science approach,* where detailed investigations are made by applying sophisticated surface science techniques to single crystal surfaces, often under well-controlled, high vacuum conditions as well-defined models of catalysts, can provide fundamental microscopic insight into the principles underlying the elementary steps of heterogeneous catalysis. As a fairly new technique used in catalysis, the STM enables a direct atomic-scale view of active sites with a low density such as edges, kinks or atomic defects, which in many cases turn out to dominate the catalytic properties. Atomic-scale insight is essential, and the STM is an excellent tool to resolve such issues on nanoclusters deposited on conducting substrates. However, one should be aware that catalyst model systems may differ significantly from the real high surface area catalysts, both with regards to the nature of the surface morphology and to the applied pressure range. Today different routes are being developed to overcome both the material and pressure gaps, and it is very likely that the STM will play a central part in this progress. The STM is limited to the study of conducting surfaces and can, e.g., not be used for the study of poorly conducting or insulating materials such as the oxide-supports widely used in catalysis. For this purpose the atomic force microscope (AFM) is a well-suited instrument, capable of probing, conducting as well as insulating surfaces, with a high degree of detail similar to STM [62,63]. In addition, a great number of new developments of the STM and related techniques are under way operating at high pressures or with high scanning speeds [64–69], and they have already shown promising results with clear significance for the fundamental studies of catalysis.

Acknowledgements

This paper is dedicated to Jens Rostrup Nielsen and Henrik Topsøe in connection with the Symposium ‘‘Frontiers in Catalysis’’ to celebrate 40 years in catalysis (JRN) and 60 years birthday (HET). We and in particular FB thank them both for a very fruitful and stimulating collaboration and for their year-long support of the STM activities at the University of Aarhus. We also gratefully acknowledge the large number of colleagues who, at different stages, have been involved in the presented work: M. Bollinger, I. Chorkendorff, B.S. Clausen, S. Dahl, B. Hammer, K. Honkala, S. Helveg, E. Lægsgaard, M. Nyberg, J.K. Nørskov, J. Schnadt, I. Stensgaard, H. Topsøe, and E.K. Vestergaard. Finally J.V.L acknowledges the financial support from the Carlsberg Foundation.

References

[1] J.W. Niemantsverdriet, Spectroscopy in Catalysis, second ed., Wiley-VCH Verlag GmbH, Weinheim, 2000.
[2] G.A. Somorjai, Surface Chemistry and Catalysis, Wiley, New York, 1994.
[3] G. Ertl, H. Knözinger, J. Weitkamp (Eds.), Handbook of Heterogeneous Catalysis, vol. 1–5, VCH, Weinheim, 1997.
[4] H. Topsøe, Stud. Surf. Sci. Catal. 130 (2000) 1.
[5] G. Binnig, H. Rohrer, Rev. Mod. Phys. 59 (1987) 615.
[6] F. Besenbacher, Rep. Prog. Phys. 59 (1996) 1737.
[7] J.C. Chen, Introduction to Scanning Tunneling Microscopy, Oxford University Press Inc., Oxford, 1993.
[8] R. Wiesendanger, Scanning Probe Microscopy and Spectroscopy, Cambridge University Press, Cambridge, 1994.
[9] J. Wintterlin, Adv. Catal. 45 (2000) 131.
[10] R. Schaub, E. Wahlström, A. Rønnau, E. Lægsgaard, I. Stensgaard, F. Besenbacher, Science 299 (2003) 377.
[11] H. Over, Y.D. Kim, A.P. Seitsonen, S. Wendt, E. Lundgren, M. Schmid, P. Varga, A. Morgante, G. Ertl, Science 287 (2000) 1474.
[12] T. Zambelli, J.V. Barth, J. Wintterlin, G. Ertl, Nature 390 (1997) 495.
[13] H. Topsøe, B.S. Clausen, F.E. Massoth, in: J.R. Anderson, M. Boudart (Eds.), Hydrotreating Catalysis, Science and Technology, vol. 11, Springer Verlag, Berlin, 1996.
[14] R. Prins, in: G. Ertl, H. Knözinger, J. Weitkamp (Eds.), Handbook of Heterogeneous Catalysis, VHC, Weinheim, 1997, p. 1908.
[15] D.D. Whitehurst, T. Isoda, I. Mochida, Adv. Catal. 42 (1998) 345.
[16] T. Kabe, A. Ishihara, W. Qian, Hydrodesulfurization and Hydrogenation—Chemistry and Engineering, Wiley-VCH, Kodansha, 1999.

[17] J.W. Gosselink, Cattech 4 (1998) 127.
[18] T.G. Parham, R.P. Merrill, J. Catal. 85 (1984) 295.
[19] B.S. Clausen, B. Lengeler, R. Candia, J. Als-Nielsen, H. Topsøe, Bull. Soc. Chim. Belg. 90 (1981) 1249.
[20] M. Boudart, R.A. Dalla Batta, K. Foger, D.G. Löffler, M.G. Samant, Science 228 (1985) 717.
[21] H. Topsøe, B.S. Clausen, Catal. Rev. Sci. Eng. 26 (1984) 395.
[22] M. Salmeron, G.A. Somorjai, A. Wold, R. Chianelli, K.S. Liang, Chem. Phys. Lett. 90 (1982) 105.
[23] J.V. Barth, H. Brune, G. Ertl, R. Behm, Phys. Rev. B 42 (1990) 9307.
[24] S. Helveg, J.V. Lauritsen, E. Lægsgaard, I. Stensgaard, J.K. Nørskov, B.S. Clausen, H. Topsøe, F. Besenbacher, Phys. Rev. Lett. 84 (2000) 951.
[25] J.V. Lauritsen, S. Helveg, E. Lægsgaard, I. Stensgaard, B.S. Clausen, H. Topsøe, F. Besenbacher, J. Catal. 197 (2001) 1.
[26] J. Tersoff, D.R. Hamann, Phys. Rev. B 31 (1985) 805.
[27] K.K. Kam, B.A. Parkinson, J. Phys. Chem. 86 (1982) 463.
[28] M.V. Bollinger, J.V. Lauritsen, K.W. Jacobsen, J.K. Nørskov, S. Helveg, F. Besenbacher, Phys. Rev. Lett. 87 (2001) 196803.
[29] M.V. Bollinger, K.W. Jacobsen, J.K. Nørskov, Phys. Rev. B 67 (2003) 085410.
[30] J.V. Lauritsen, M. Nyberg, J.K. Nørskov, B.S. Clausen, H. Topsøe, E. Lægsgaard, F. Besenbacher, J. Catal. 224 (2004) 94.
[31] J.V. Lauritsen, M. Nyberg, R.T. Vang, M.V. Bollinger, B.S. Clausen, H. Topsøe, K.W. Jacobsen, F. Besenbacher, E. Lægsgaard, J.K. Nørskov, F. Besenbacher, Nanotechnology 14 (2003) 385.
[32] W. Niemann, B.S. Clausen, H. Topsøe, Catal. Lett. 4 (1990) 355.
[33] S.P.A. Louwers, R. Prins, J. Catal. 133 (1992) 94.
[34] S.M.A.M. Bouwens, J.A.R. van Veen, D.C. Koningsberger, V.H.J. de Beer, R. Prins, J. Phys. Chem. 95 (1991) 123.
[35] L.S. Byskov, J.K. Nørskov, B.S. Clausen, H. Topsøe, J. Catal. 187 (1999) 109.
[36] P. Raybaud, J. Hafner, G. Kresse, S. Kasztelan, H. Toulhoat, J. Catal. 190 (2000) 128.
[37] B. Hinnemann, J.K. Nørskov, H. Topsøe, J. Phys. Chem. B 109 (2005) 2245.
[38] P. Zeuthen, L. Skyum, Hydrocarbon Eng. 11 (2004) 65.
[39] H. Topsøe, B. Hinnemann, J.K. Nørskov, J.V. Lauritsen, F. Besenbacher, P.L. Hansen, G. Hytoft, R.G. Egeberg, K.G. Knudsen, Catal. Today 107–108 (30 October 2005) 12–22.
[40] J.R. Rostrup-Nielsen, J. Sehested, J.K. Norskov, Adv. Catal. 47 (2002) 65.
[41] J.R. Rostrup-Nielsen, in: J.R. Anderson, M. Boudart (Eds.), CATALYSIS—Science and Technology, Springer-Verlag, Berlin, 1984, p. 1.
[42] J.R. Rostrup-Nielsen, T. Rostrup-Nielsen, CATTECH 6 (2002) 150.
[43] S. Helveg, C. Lopez-Cartes, J. Sehested, P.L. Hansen, B.S. Clausen, J.R. Rostrup-Nielsen, F. Abild-Pedersen, J.K. Nørskov, Nature 427 (2004) 426.
[44] H.S. Bengaard, J.K. Norskov, J. Sehested, B.S. Clausen, L.P. Nielsen, A.M. Molenbroek, J.R. Rostrup-Nielsen, J. Catal. 209 (2002) 365.
[45] J.R. Rostrup-Nielsen, J. Catal. 85 (1984) 31.
[46] V. Ponec, Appl. Catal. A 222 (2001) 31.
[47] J.H. Sinfelt, Bimetallic Catalysts, Discoveries, Concepts and Applications, Wiley, New York, 1983.
[48] L.P. Nielsen, F. Besenbacher, I. Stensgaard, E. Lægsgaard, C. Engdahl, P. Stoltze, K.W. Jacobsen, J.K. Nørskov, Phys. Rev. Lett. 71 (1993) 754.
[49] F. Besenbacher, L.P. Nielsen, P.T. Sprunger, Chemical Physics of Solid Surfaces and Heterogeneous Catalysis, Elsevier Science Publishers, 1997 (Chapter 10).
[50] J. Jacobsen, L.P. Nielsen, F. Besenbacher, I. Stensgaard, E. Lægsgaard, T. Rasmussen, K.W. Jacobsen, J.K. Nørskov, Phys. Rev. Lett. 75 (1995) 489.
[51] F. Besenbacher, I. Chorkendorff, B.S. Clausen, B. Hammer, A.M. Molenbroek, J.K. Nørskov, I. Stensgaard, Science 279 (1998) 1913.
[52] B. Hammer, private communication.
[53] T. Zambelli, J. Wintterlin, J. Trost, G. Ertl, Science 273 (1996) 1688.
[54] S. Dahl, A. Logadottir, R.C. Egeberg, J.H. Larsen, I. Chorkendorff, E. Törnquist, J.K. Nørskov, Phys. Rev. Lett. 83 (1999) 1814.
[55] J.K. Nørskov, T. Bligaard, A. Logadottir, S. Bahn, L.B. Hansen, M. Bollinger, H. Bengaard, B. Hammer, Z. Sljivancanin, M. Mavrikakis, Y. Xu, S. Dahl, C.J.H. Jacobsen, J. Catal. 209 (2002) 275.
[56] Z.P. Liu, P. Hu, J. Am. Chem. Soc. 125 (2003) 1958.
[57] T. Zubkov, G.A. Morgan Jr., J.T. Yates Jr., O. Kühlert, M. Lisowski, R. Schillinger, D. Fick, H.J. Jänsch, Surf. Sci. 526 (2003) 57.
[58] P. Gambardella, Z. Sljivancanin, B. Hammer, M. Blanc, K. Kuhnke, K. Kern, Phys. Rev. Lett. 87 (2001) 056103.
[59] I.M. Ciobicã, R.A. van Santen, J. Phys. Chem. B 107 (2003) 3808.
[60] R.T. Vang, K. Honkala, S. Dahl, E.K. Vestergaard, J. Schnadt, E. Lægsgaard, B.S. Clausen, J.K. Nørskov, F. Besenbacher, Nat. Mater. 4 (2005) 160.
[61] D.W. Goodman, Surf. Sci. Lett. 105 (1981) L265.
[62] C. Barth, M. Reichling, Nature 414 (2001) 54.
[63] Y. Namai, K.-I. Fukui, Y. Iwasawa, Catal. Today 85 (2003) 79.
[64] B.L.M. Hendriksen, J.W.M. Frenken, Phys. Rev. Lett. 89 (2002) 046101.
[65] P. Thostrup, E.K. Vestergaard, T. An, E. Laegsgaard, F. Besenbacher, J. Chem. Phys. 118 (2003) 3724.
[66] L. Österlund, P.B. Rasmussen, P. Thostrup, E. Lægsgaard, I. Stensgaard, F. Besenbacher, Phys. Rev. Lett. 86 (2001) 460.
[67] A. Kolmakov, D.W. Goodman, Rev. Sci. Instrum. 74 (2003) 2444.
[68] M. Rössler, P. Geng, J. Wintterlin, Rev. Sci. Instrum. 76 (2005) 023705.
[69] M.J. Rost, L. Crama, P. Schakel, E. van Tol, G. van Velzen-Williams, C.F. Overgauw, H. ter Horst, H. Dekker, B. Okhuijsen, M. Seynen, A. Vijftigschild, P. Han, A.J. Katan, K. Schoots, R. Schumm, W. van Loo, T.H. Oosterkamp, J.W.M. Frenken, Rev. Sci. Instrum. 76 (2005).